Molecular Crystals and Liquid Crystals Science and Technology. Section A. Molecular Crystals and Liquid Crystals

Publication details, including instructions for authors and subscription information:
http://www.tandfonline.com/loi/gmcl19

Crystal Structures, Magnetic Structures and Photophysics in Supramolecular Transition-Metal Oxalate Compounds

Silvio Decurtins [a] , Helmut W. Schmalle [a] , Rene Pellaux [a] , Peter Fischer [b] & Andreas Hauser [c]

[a] Institut für Anorganische Chemie, Universität Zürich, Switzerland

[b] Laboratorium für Neutronenstreuung, ETH/PSI, Villigen, Switzerland

[c] Institut für Anorganische Chemie, Universität Bern, Switzerland

Version of record first published: 04 Oct 2006

To cite this article: Silvio Decurtins, Helmut W. Schmalle, Rene Pellaux, Peter Fischer & Andreas Hauser (1997): Crystal Structures, Magnetic Structures and Photophysics in Supramolecular Transition-Metal Oxalate Compounds, Molecular Crystals and Liquid Crystals Science and Technology. Section A. Molecular Crystals and Liquid Crystals, 305:1, 227-237

To link to this article: http://dx.doi.org/10.1080/10587259708045060

Mol. Cryst. Liq. Cryst., 1997, Vol. 305, pp. 227–237
Reprints available directly from the publisher
Photocopying permitted by license only

CRYSTAL STRUCTURES, MAGNETIC STRUCTURES AND PHOTOPHYSICS IN SUPRAMOLECULAR TRANSITION-METAL OXALATE COMPOUNDS

SILVIO DECURTINS,[1] HELMUT W. SCHMALLE,[1] RENE PELLAUX,[1] PETER FISCHER,[2] ANDREAS HAUSER[3]
[1]Institut für Anorganische Chemie, Universität Zürich, Switzerland;
[2]Laboratorium für Neutronenstreuung, ETH/PSI, Villigen, Switzerland;
[3]Institut für Anorganische Chemie, Universität Bern, Switzerland

Abstract Polymeric two- and three-dimensional, homo- and heterometallic oxalate-bridged coordination compounds offer exciting opportunities, mainly in the fields of molecular magnetism and photophysics. Given that a large variety of magnetic phenomena have been reported so far from these molecular magnets, very limited experience is gained from elastic neutron scattering experiments. Therefore, with two examples, we will address the topic of the elucidation of magnetic structures by means of the neutron scattering technique. In addition, due to the possibility of the variation of different metal ions in varying oxidation states, interesting photophysical processes can be observed within the extended three-dimensional host/guest systems.

INTRODUCTION

The design of synthetic pathways to chemical systems of desired properties continues to be a challenge for the preparative chemists. In this context, a great deal of interest has been devoted to the development of rational synthetic routes to novel one- to three-dimensional, polymeric coordination compounds which have applications as molecular-based magnetic materials.

In that field, a successful molecular design of metal-complex magnets which are based on trioxalatochromium(III) building blocks, has been reported in 1992.[1] Within a series of layered, oxalate-bridged bimetallic compounds, ferromagnetic ordering behavior has been shown to occur at temperatures < 14 K. Since then, a variety of analogous two-dimensional (2D), bimetallic assemblies, also with mixed-valency stoichiometries, have been prepared and characterized.[2-8] Overall, many of these layered compounds exhibit ferro-, ferri- or antiferromagnetic long-range ordering behavior and in some cases they show at least evidence for short-range interactions. Furthermore, as an extension to the structurally two-dimensional compounds, it seemed likely, that also three-dimensionally-bridged metal assemblies could be realised. Accordingly, on the basis of a chiral

template, namely a tris-bipyridine transition-metal complex, three-dimensional (3D), homo- and heterometallic oxalate-bridged frameworks have been synthesized.[9-11] As expected, these supramolecular host/guest compounds reveal an interesting structural topology, and in addition, many of them show a long-range magnetic ordering behavior as well as various kinds of photophysical properties.

Given that an astonishing diversity of magnetic phenomena is generated by these polymeric 2D and 3D framework compounds and that a large body of experimental results is reported from magnetic susceptibility and magnetization studies, very limited experience has been gained so far from elastic neutron scattering experiments aimed at elucidating the spin structure in the magnetically ordered state. Therefore, this report intends to describe some results of neutron scattering experiments with the 2D and 3D oxalate-bridged transition-metal compounds.[8,11]

Finally, an overview about possible photophysical processes occurring in the 3D supramolecular host/guest compounds is presented. Thereby, we address the basic idea in the field of molecular magnetism, namely to engineer novel molecular compounds that are not only magnetic but which also possess additional characteristics, for instance in the field of photophysics.[10,12]

STRUCTURAL PROPERTIES

Basic Principles

The oxalate ion, $C_2O_4^{2-}$, is well known to be an attractive ligand, because its ambidentate coordinating ability enables the construction of homo- and bimetallic chain- and layer-structures, and even the formation of three-dimensionally connected transition-metal frameworks. In the following, we will discuss some basic ideas which are relevant for the understanding of the two- and three-dimensional framework topologies. Both structure types are formally composed of $[M^{z+}(ox)_3]^{(6-z)-}$ building blocks, whereby each of these units represents a three-connected point. These subunits which are predestined to create extended network motifs, may polymerise in principle in two ways. Thereby, one alternative leads to a 2D honeycomb layer compound, whereas in the other possible arrangement, an infinite 3D structure is formed. In the former case, building blocks of different chirality are alternately linked and consequently, the bridged metal ions are confined to lie within a plane, as it is illustrated in Figure 1a. Consequently, a layered structure motif will result. In contrast, as it is depicted in Figure 1b, an assembling of building blocks of the same chiral configuration will lead to a 3D framework structure.

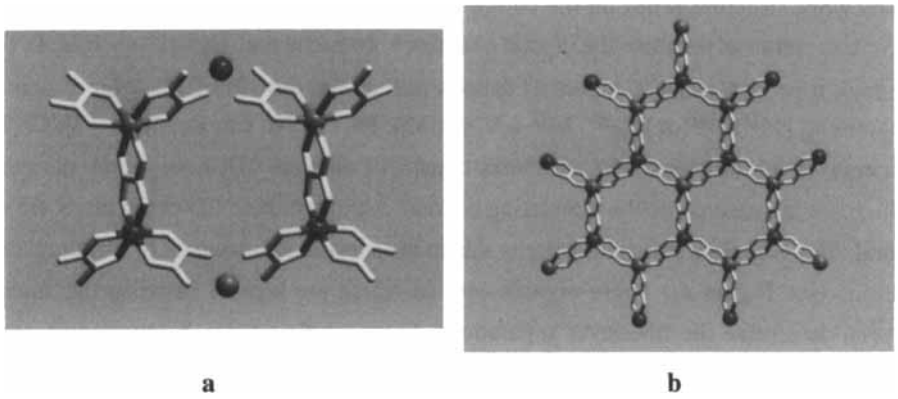

FIGURE 1: Chiral $[M^{z+}(ox)_3]^{(6-z)-}$ building blocks assembled with a) alternating chiral configuration, b) equal chiral configuration.

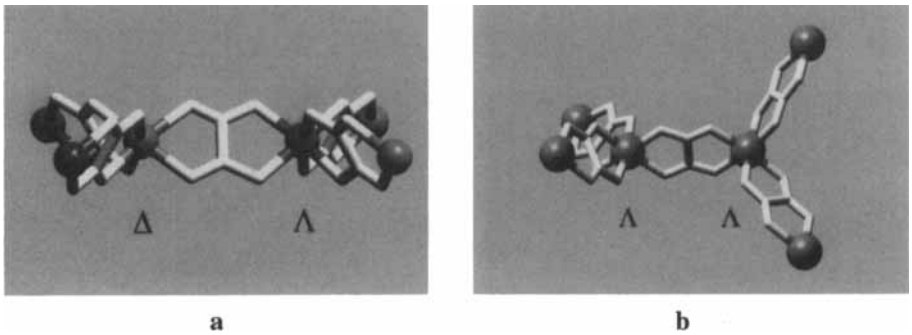

FIGURE 2: a) Two dimeric units of the alternating chirality type are necessary to form a closed hexa-gon ring; b) the resulting planar network motif.

As a next step, simple topological rules will be applied in order to define the number of subunits which are needed to build closed circuits, hence, extended framework motifs. Figure 2 illustrates the way that two dimeric subunits may be combined to form the planar honeycomb network. In an analogous manner, it can easily be seen from Figure 3, that two tetrameric subunits are needed to build closed circuits composed of ten metal centers, which in sum define the three-dimensional decagon framework structures.

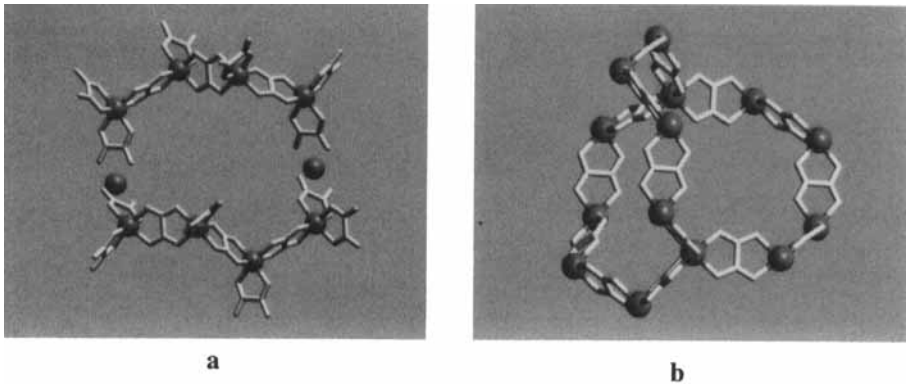

a b

FIGURE 3: a) Two tetrameric units of the same chirality type are necessary to form a closed deca-gon ring; b) a fragment of the 3D, chiral framework.

The Honeycomb Layer Structure

The discrimination between the formation and crystallization either of a 2D or a 3D framework structure relies on the choice of the templating counterion. Evidently, the template cation determines the crystal chemistry. In particular, $[XR_4]^+$ (X = N, P; R = phenyl, n-propyl, n-butyl, n-pentyl) cations initiate the growth of 2D layer structures containing $[M^{II}M^{III}(ox)_3]_n^{n-}$, M^{II} = V, Cr, Mn, Fe, Co, Ni, Cu, Zn; M^{III} = V, Cr, Fe, network stoichiometries. The structures consist of anionic, 2D, honeycomb networks which are interleaved by the templating cations. Although these 2D compounds are not chiral, they express a structural polarity due to the specific arrangement of the templating cations (see Figure 4). These organic cations which are located between the anionic layers, determine the interlayer separations. From single-crystal X-ray studies, these distances have been determined to the values 9.94 Å, 9.55 Å, 8.91 Å, and 8.20 Å for the n-pentyl, phenyl, n-butyl, and n-propyl derivatives.[2,3,6,8]

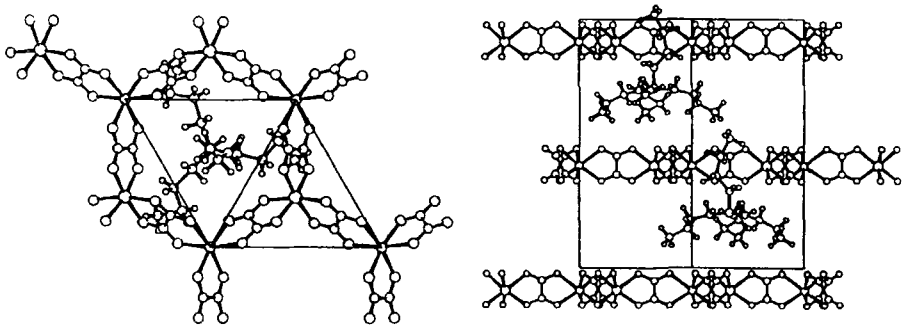

a b

FIGURE 4: Sector from the $[N(n\text{-butyl})_4][Mn^{II}Fe^{III}(ox)_3]$ layer compound. a) [001] projection; b) [110] projection.[8]

The Chiral 3D Host/Guest System

The cationic, tris-chelated transition-metal diimine complexes, $[M(bpy)_3]^{2+/3+}$, act as templates for the formation and crystallization of the 3D deca-gon framework structures.[9-11] As outlined above, the topological principle implies for the 3D case, that only subunits of the same chiral configuration are assembled. Consequently, the uniform anionic 3D network-type with stoichiometries like $[M^{II}_2(ox)_3]_n^{2n-}$, $[M^{I}M^{III}(ox)_3]_n^{2n-}$ or $[M^{II}M^{III}(ox)_3]_n^{n-}$ is chiral, as it is composed of 2n centers exhibiting the same kind of chirality. Naturally, this chiral topology is in line with the symmetry elements which are present in the crystalline state of the 3D frameworks, which in sum constitute either one of the enantiomorphic cubic space groups $P4_332$ or $P4_132$ for the former and the cubic space group $P2_13$ for the latter bimetallic stoichiometries. Thereby, the 2n metal ions occupy special sites with a three-fold symmetry axis. Figure 5 depicts a stereo view of the decagon network topology.

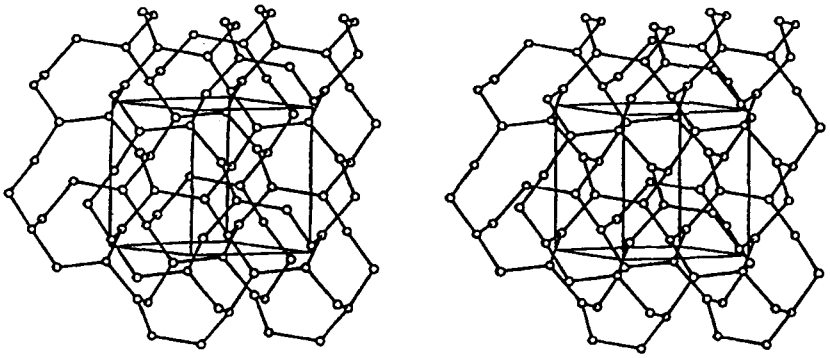

FIGURE 5: Stereo view of the 3-connected 10-gon (10,3) network topology.

MAGNETIC PROPERTIES AND MAGNETIC STRUCTURES

A 2D Ferromagnet

The layer compound with stoichiometry $[A][Mn^{II}Cr^{III}(ox)_3]$, is known to exhibit a transition to a ferromagnetically ordered state at $T_C = 6$ K.[1-3,8] A single-crystal field-dependent magnetization experiment with the compound $[N(n\text{-propyl})_4][Mn^{II}Cr^{III}(ox)_3]$, revealed a distinct anisotropic behavior such that the easy-axis of magnetization is lying predominantly in the direction of the c-axis, thus perpendicular to

the hexagonal network.[8] As it is illustrated in Figure 6, with the parallel orientation of the external field to the c-axis, the saturation is reached in a field of H ≈ 0.1 T, while the saturation field in the perpendicular direction is H > 0.3 T. This finding is in accordance with the results of the neutron scattering experiment s(vide infra).

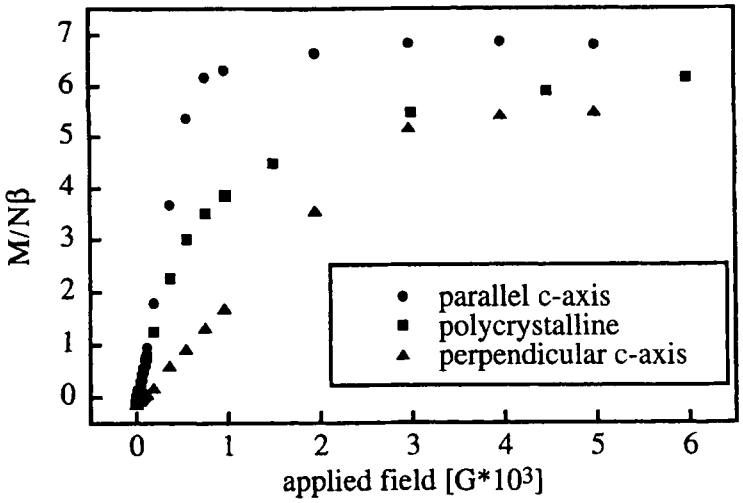

FIGURE 6: Plot of the field dependence of the magnetization for a single-crystal of $[N(n\text{-propyl})_4][Mn^{II}Cr^{III}(ox)_3]$ at T = 4.2 K.

In order to verify the magnetic long-range ordering character below T_C = 6 K, and to elucidate experimentally the magnetic structure of that ferromagnetic compound, an elastic neutron scattering study was undertaken with a polycrystalline sample with $A^+ = [P(C_6D_5)_4]^+$.[8] First, the structural part of the diffraction pattern had to be examined from room-temperature down to liquid-helium temperatures. Figure 7 shows a profile matching of a 1.8 K neutron diffraction pattern of the polycrystalline sample. The refined unit cell parameters within space group R32 show the values a=b=18.749(3) Å, c=111.89(3) Å. The c-axis was formerly determined from a single-crystal X-ray measurement at room-temperature within space group R3c to a value of c=57.283(24) Å.[3] The doubling of the c-axis as a result from the refinement of the neutron diffraction pattern, is interpreted to originate either from a superstructure phenomenon or from a twinning effect.

Furthermore, as anticipated from the magnetic susceptibility data, a difference in the peak intensities due to long-range ferromagnetic ordering of the magnetic moments from the Mn^{2+} and Cr^{3+} ions could be detected from the neutron diffraction experiment

at the temperatures 1.8 K and 12 K. Figure 8 illustrates the observed [difference I(1.8 K) - I(12 K)] and calculated magnetic neutron diffraction patterns. Thereby it has to be noted, that the increase of the intensities corresponds to a propagation vector **K** = 0. The temperature dependence of the dominant magnetic intensity at $2\Theta = 69{,}1°$ indicates an ordering temperature of 6.0(5) K, in good agreement with the magnetic susceptibility measurements. The observed enhancement in some of the Bragg reflections proves the presence of long-range magnetic interactions within this structurally two-dimensional compound. Finally, the best agreement between observed and calculated neutron intensities was achieved with a collinear ferromagnetic arrangement of both the Mn^{2+} and Cr^{3+} spins along the c-axis.

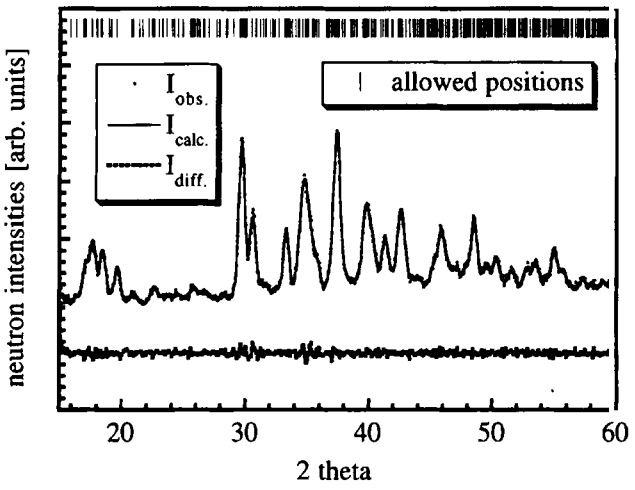

FIGURE 7: Observed neutron diffraction pattern of a polycrystalline sample of $[P(C_6D_5)_4][Mn^{II}Cr^{III}(ox)_3]$ at T = 1.8 K with the profile matching plot for space group R32. λ = 2.398 Å.

A 3D Antiferromagnet

The existence of a magnetically ordered phase for the compound $[Fe(bpy)_3][Mn^{II}_2(ox)_3]$ could be deduced from magnetic susceptibility measurements, which revealed a rounded maximum at about 20 K in the χ_M versus T curve (thus $T_N < 20$ K) as well as a Weiss constant Θ of -33 K in the $1/\chi_M$ versus T plot.[9] As anticipated, an increase of the intensities due to long-range antiferromagnetic ordering of the spins from the Mn^{2+} ions could be detected with the neutron diffraction experiments performed in the temperature range from 30 K to 1.8 K with a deuterated polycrystalline sample.[11] Figure 9 illustrates

the observed [difference I(1.8 K) - I(30 K)], calculated and difference magnetic neutron diffraction patterns. The increase of the intensities corresponds to a propagation vector **K** = 0, thus the magnetic unit cell is equal to the chemical cell.

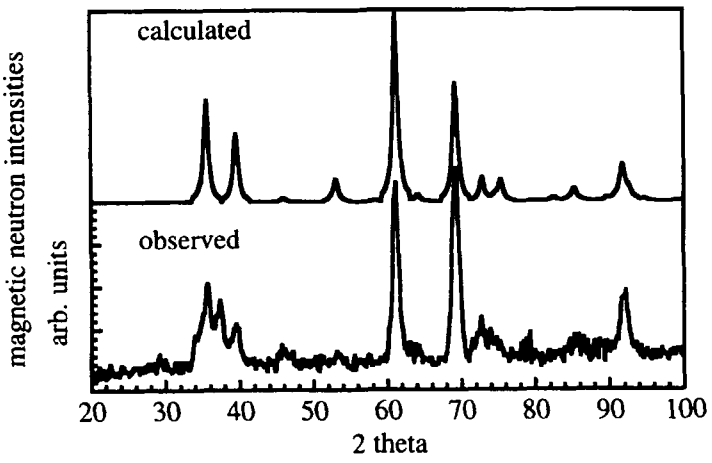

FIGURE 8: Observed [difference I(1.8 K) - I(12 K)] and calculated magnetic neutron diffraction patterns of a polycrystalline sample of $[P(C_6D_5)_4][Mn^{II}Cr^{III}(ox)_3]$; $\lambda = 4.766$ Å. The calculation is based on a ferromagnetic spin configuration parallel to the c-axis.

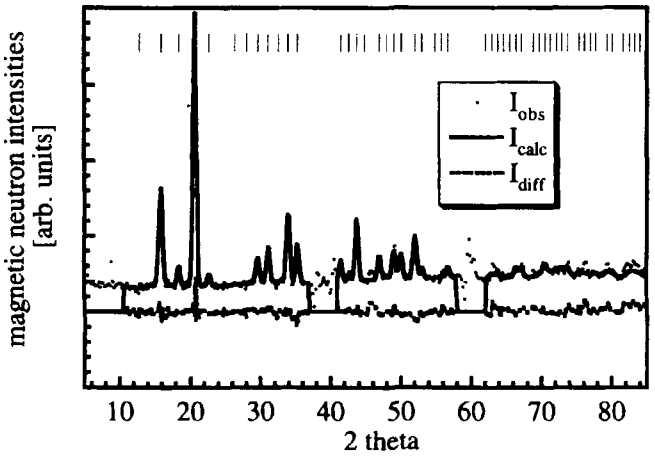

FIGURE 9: Observed [difference I(1.8 K) - I(30 K)], calculated and difference magnetic neutron diffraction patterns of a polycrystalline sample of $[Fe^{II}(d_8\text{-bpy})_3][Mn^{II}{}_2(ox)_3]$; $\lambda = 2.5154$ Å.

The best agreement between observed and calculated magnetic neutron intensities was achieved with a collinear, antiferromagnetic arrangement of the Mn^{2+} moments, thus a two-sublattice spin configuration has been proven to occur.

PHOTOPHYSICAL PROPERTIES

Chemical variation and combination of metal ions of different valencies in the oxalate backbone of the two- and three-dimensionally bridged frameworks as well as in the tris-bipyridine cations offer unique opportunities for studying a large variety of photophysical processes, such as light-induced electron transfer and excitation energy transfer in the solid state.[10,12] In this report we will comment on some observations of the excitation energy transfer processes within the 3D, supramolecular host/guest compounds. Depending upon the relative energies of the excited states of the chromophores, energy transfer is observed either from the guest system with the tris-bipyridine cations as donors to the host system where the oxalate-backbone acts as acceptor sites or vice versa. In addition, energy migration, that is excitation energy transfer between identical chromophores, occurs within the host as well as within the guest system.[12] The following stoichiometries $[Ru_{1-x}Os_x(bpy)_3][NaAl(ox)_3]$ and $[Ru(bpy)_3][NaAl_{1-x}Cr_x(ox)_3]$ are chosen to illustrate with examples these specific photophysical properties.

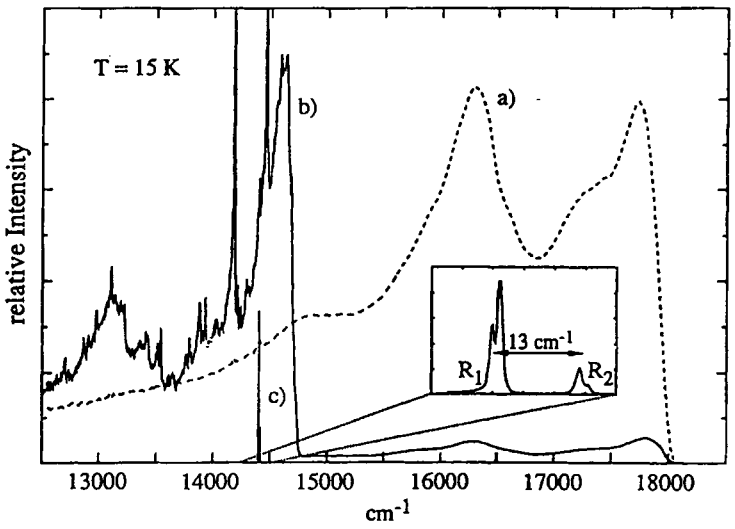

FIGURE 10: Luminescence spectra at T = 15 K of a) $[Ru(bpy)_3][NaAl(ox)_3]$; b) $[Ru_{1-x}Os_x(bpy)_3][NaAl(ox)_3]$, x=1 %; c) $[Ru(bpy)_3][NaCr(ox)_3]$; λ=476 nm.

Figure 10 shows the luminescence spectra of three representative compounds. If Al^{3+} is replaced by Cr^{3+}, the $[Ru(bpy)_3]^{2+}$ luminescence from the spin-forbidden MLCT transition is completely quenched and the sharp luminescence bands characteristic for the zero-field components of the $^2E \rightarrow {}^4A_2$ transition of octahedrally coordinated and trigonally distorted Cr^{3+} are observed at 14'400 cm^{-1}.This is a clear indication for very efficient energy transfer from the initially excited $[Ru(bpy)_3]^{2+}$ to $[Cr(ox)_3]^{3-}$.

Not only acceptors on the oxalate backbone may quench the $[Ru(bpy)_3]^{2+}$ luminescence. Replacing a fraction of the $[Ru(bpy)_3]^{2+}$ by $[Os(bpy)_3]^{2+}$ results in luminescence from $[Os(bpy)_3]^{2+}$ and a quenching of the $[Ru(bpy)_3]^{2+}$ luminescence, too. Indeed, the energy transfer to $[Os(bpy)_3]^{2+}$ is even more efficient than to $[Cr(ox)_3]^{3-}$. This is due to the higher oscillator strength of the MLCT absorption on $[Os(bpy)_3]^{2+}$ as compared to the spin allowed d-d transition on $[Cr(ox)_3]^{3-}$. Figure 11 summarizes within a schematic representation these different photophysical processes.

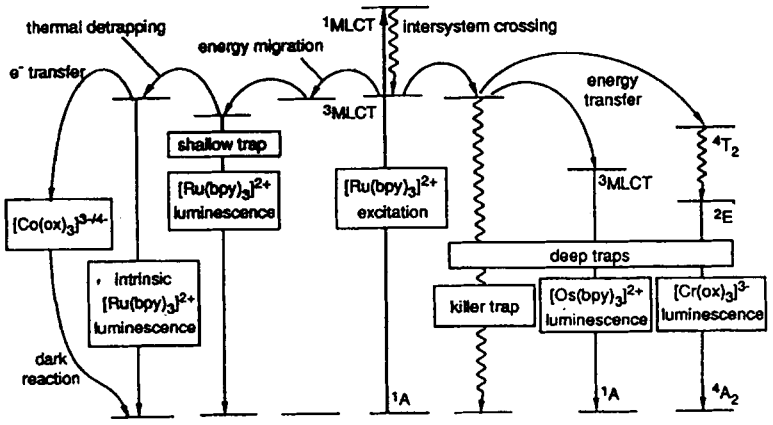

FIGURE 11: Schematic representation of different photophysical processes observed in $[Ru_{1-x}Os_x(bpy)_3][NaAl(ox)_3]$ and $[Ru(bpy)_3][NaAl_{1-x}Cr_x(ox)_3]$.

PERSPECTIVES

In conclusion, the outlined results of the neutron diffraction experiments have successfully proven to trace the spin configuration defining the antiferromagnetic and ferromagnetic phases in 3D and 2D molecular framework compounds. The short comment on the photophysical energy transfer processes within the 3D compounds points to another exciting aspect in the study of molecular-based magnetic materials.

ACKNOWLEDGMENT

Financial support by the Swiss National Science Foundation is acknowledged.

REFERENCES

1. H. Tamaki, Z. J. Zhong, N. Matsumoto, S. Kida, M. Koikawa, N. Achiwa, Y. Hashimoto, and H. Okawa, J. Am. Chem. Soc., 114, 6974 (1992).
2. L. O. Atovmyan, G. V. Shilov, R. N. Lyubovskaya, E. I. Zhilyaeva, N. S. Ovanesyan, S. I. Pirumova, and I. G. Gusakovskaya, JETP Lett., 58, 766 (1993).
3. S. Decurtins, H. W. Schmalle, H. R. Oswald, A. Linden, J. Ensling, P. Gütlich, and A. Hauser, Inorg. Chim. Acta, 216, 65 (1994).
4. W. M. Reiff, J. Kreisz, L. Meda, and R. U. Kirss, Mol. Cryst. Liq. Cryst., 273, 181 (1995).
5. C. Mathonière, C. J. Nuttall, S. G. Carling, and P. Day, Inorg. Chem., 35, 1201 (1996).
6. S. G. Carling, C. Mathonière, P. Day, K. M. A. Malik, S. J. Coles, and M. B. Hursthouse, J. Chem. Soc., Dalton Trans., 1839 (1996).
7. A. Bhattacharjee, S. Iijima, and F. Mitzutani, J. Magn. Magn. Mater., 153, 235 (1996).
8. R. Pellaux, H. W. Schmalle, R. Huber, P. Fischer, T. Hauss, and S. Decurtins, Inorg. Chem., submitted.
9. S. Decurtins, H. W. Schmalle, P. Schneuwly, J. Ensling, and P. Gütlich, J. Am. Chem. Soc., 116, 9521 (1994).
10. S. Decurtins, H. W. Schmalle, R. Pellaux, P. Schneuwly, and A. Hauser, Inorg. Chem., 35, 1451 (1996).
11. S. Decurtins, H. W. Schmalle, R. Pellaux, R. Huber, P. Fischer, and B. Ouladdiaf, Adv. Mater., in press.
12. M. E. von Arx, A. Hauser, H. Riesen, R. Pellaux, and S. Decurtins, Phys. Rev. B, submitted.